




Convex-roof entanglement measures of density matrices block diagonal in disjoint subspaces for the study of thermal states

Mikołaj Jędrzejewski ¹, Kacper Kinastowski ¹ and Katarzyna Roszak ^{2,1}

¹*Department of Theoretical Physics, Faculty of Fundamental Problems of Technology, Wrocław University of Science and Technology, 50-370 Wrocław, Poland*

²*Department of Optics, Palacký University, 17 Listopadu 12, 771 46 Olomouc, Czech Republic*



(Received 25 February 2022; revised 19 May 2022; accepted 24 May 2022; published 13 June 2022)

We provide a proof that entanglement of any density matrix which is block diagonal in subspaces which are disjoint in terms of the Hilbert space of one of the two potentially entangled subsystems can simply be calculated as the weighted average of entanglement present within each block. This is especially useful for thermal-equilibrium states which always inherit the symmetries present in the Hamiltonian, since block-diagonal Hamiltonians are common, as are interactions which involve only a single degree of freedom of a greater system. We exemplify our method on a simple Hamiltonian, showing the diversity in possible temperature dependences of Gibbs state entanglement which can emerge in different parameter ranges.

DOI: [10.1103/PhysRevA.105.062419](https://doi.org/10.1103/PhysRevA.105.062419)

I. INTRODUCTION

The quantification of entanglement for mixed states is a complicated problem, especially once the system under study becomes larger. This is reflected in the number of entanglement measures which have been proposed and are used to date and the fact that no unique entanglement measure for mixed states has been established [1]. Each comes with its own set of problems, which can be broadly classified as either the need of numerical optimization of complex functions over a set of parameters which grows rapidly with system size or the inability to detect certain types of entanglement. The first is characteristic of measures such as distillable entanglement [2–5], entanglement cost [6], and all convex-roof entanglement measures, such as entanglement of formation (EoF) [2,7]. Negativity [8–10], on the other hand, is much easier to compute, since it requires only diagonalization, but it has no clear physical interpretation and it suffers from the second drawback, since it cannot detect bound entangled states [11–17]. Bound entangled states can occur only for systems of product dimension larger than 6 in the case of bipartite systems [18], so they are a small problem unless systems are relatively large, but they have been found already for very mixed states of two qutrits [11].

The quest to find efficiently computable entanglement measures that have a clear physical interpretation continues [19–21], because entanglement remains an important factor which predetermines the possibility of very quantum and nonintuitive behavior of bipartite systems. One approach is to sacrifice generality in order to obtain solvable scenarios, which allows for the study of entanglement present in density matrices generated by a certain class of Hamiltonians. This has been done for qubits interacting with large environments via a Hamiltonian, which leads to qubit pure decoherence [19,22,23], and then generalized to systems of any size [24]. The result here was that increased understanding

of this type of entanglement enabled schemes for its measurement to be devised [25–27], which have been experimentally tested [28].

We will be focusing on the class of convex-roof entanglement measures, which are easiest to understand on an intuitive level, as they are defined by a direct extension of a good pure-state entanglement measure (concave, additive under a tensor product, and monotonic) to mixed states. They come with a seemingly straightforward instruction for computation: Calculate the mean entanglement of the state under study decomposed into pure states and then minimize over all possible decompositions. There even exists a way to find the EoF directly from the density matrix for a system of two qubits [29] and efficient minimization techniques for small bipartite systems [30]. Nevertheless, for larger systems these measures are usually not found directly using the instruction, because the number of minimization parameters grows quadratically with system size and the task quickly becomes numerically complex. Instead they are evaluated on the basis of various techniques used to make minimization efficient or to bypass it entirely. These include approximations of the lower bounds of entanglement measures [31–33], direct methods for states possessing additional symmetries [34–37], variational approaches to minimization and conjugate gradient methods [30,38,39], and the minimization over pure-state extensions of the state [40]. Another technique exchanges minimization for random sampling of possible pure-state decompositions [17,41,42]. The majority of the techniques benefit greatly from a reduction of the size of the Hilbert space of the system under study.

In our study we focus on a class of bipartite density matrices which are block diagonal in subspaces of the Hilbert space which are disjoint in terms of states of one of the two subsystems. We show that for such density matrices the convex-roof entanglement measure based on linear entropy as the pure-state measure of entanglement can be found as

the average of the amount of entanglement contained within each block. Hence the minimization has only to be performed within the disjoint subspaces separately, substantially reducing the complexity of entanglement quantification. We generalize this result to constructions based on other pure-state entanglement measures such as entanglement entropy for the special case when one subsystem is a qubit, because only then the measures are concave functions of the purity. One consequence of this from a quantum information perspective is that bound entanglement cannot transcend between such blocks. This allows criteria which disqualify the possibility of the appearance of bound entanglement to be applied to the blocks separately, thus extending the applicability of rank and system-size constraints to larger systems.

A relevant question is whether the desired structure can appear in physical systems. We mainly focus here on thermal states due to renewed interest in the context of quantum information [43–47]. Thermal states have the advantage that the symmetries within them are directly transferred from the Hamiltonian; thus if a Hamiltonian is block diagonal, the corresponding thermal state will also be block diagonal within the same subspaces. The condition for the blocks to be disjoint in terms of one subsystem is commutation of the full Hamiltonian with a nontrivial operator acting solely on this part of the system. We provide examples of such Hamiltonians stemming from solid-state physics. Incidentally, for this class of Hamiltonians also time evolution can retain the block-diagonal structure, but this requires additional restrictions to be imposed on the initial state.

We provide exemplary dependences of entanglement on temperature in Gibbs states for block-diagonal Hamiltonians, where the disjoint blocks are small enough to allow for the use of the Wootters formula [29] while the whole system is very large. This allows us to demonstrate the efficiency of the method and study the interplay of entanglement characteristics of each block within the whole state. We find that parameter changes in the Hamiltonian can lead to qualitative changes in the behavior of entanglement, some dependent on how entanglement within a given block reacts to temperature-induced mixing of the state, but most related to how the different blocks are mixed. Hence, the use of our simplified formula allows us to draw conclusions about the physics of entanglement.

The paper is organized as follows. In Sec. II we describe the class of mixed states under study and in Sec. III we briefly comment on convex-roof entanglement measures. Section IV contains the proof that calculation of measures based on linear entropy for block-diagonal density matrices of the type studied can be reduced to averaging of entanglement within separate blocks and generalizes this to other pure-state entanglement measures for the special case when one subsystem of the bipartite state is a qubit. In Sec. V we comment on the consequences of this fact from a quantum information perspective, while in Sec. VI we discuss the types of systems which will yield the desired form of the state at thermal equilibrium and during time evolution. In Sec. VI we provide a simple example and study the temperature dependence of entanglement in different parameter ranges. Section VII concludes the paper.

II. ENTANGLEMENT IN DENSITY MATRICES BLOCK DIAGONAL IN DISJOINT SUBSPACES

We are studying bipartite density matrices and for clarity we will be calling one part the quantum system (QS) and the other part the environment. This is because the density matrices under consideration are asymmetric with respect to the two subsystems and an easily made distinction is necessary.

The first assumption made about the form of the joint QS-environment (QSE) density matrices under study is that they are block diagonal in some separable QSE basis. Let us denote this basis by $\{|s\rangle\}$ for the QS and $\{|e\rangle\}$ for the environment, so the density matrix is block diagonal in the basis $\{|se\rangle \equiv |s\rangle \otimes |e\rangle\}$. We will keep the notation with QS states on the left and environmental states on the right of the ket or tensor product throughout the paper. We further assume that the block-diagonal form is the result of the properties of the environment, so each block is built of QSE states in which the whole range of QS states can be present, but the set of environmental states in each block is orthogonal to the states in any other block. Hence the class of density matrices under study can be written as

$$\hat{\rho} = \sum_n p_n \hat{\rho}_n, \quad (1)$$

where the index n distinguishes between the blocks, p_n are probabilities with $\sum_n p_n = 1$, and $\hat{\rho}_n$ are density matrices occupying disjoint blocks in terms of environment subspaces. These density matrices not only fulfill $\hat{\rho}_n \hat{\rho}_m = 0$ for $n \neq m$, but each can be written as

$$\hat{\rho}_n = \sum_{ss'} \sum_{e_n e'_n} c_{ss'}^{e e'} |s\rangle \langle s'| \otimes |e_n\rangle \langle e'_n|, \quad (2)$$

where all states $|e_n\rangle$ for a given n constitute a separate subspace of the environment so that $\langle e_n | e'_m \rangle = 0$ for all e and e' if $n \neq m$.

Let us exemplify this on the simplest possible nontrivial density matrix, when the QS is a qubit with states $|0\rangle$ and $|1\rangle$ while the environment is of dimension $N = 4$ with states $\{|0\rangle, |1\rangle, |2\rangle, |3\rangle\}$. A mixed QSE state

$$\hat{\rho} = \frac{1}{4} (|\Psi_{01}\rangle \langle \Psi_{01}| + |\Phi_{01}\rangle \langle \Phi_{01}| + |\Psi_{23}\rangle \langle \Psi_{23}| + |\Phi_{23}\rangle \langle \Phi_{23}|), \quad (3)$$

with Bell-like components

$$|\Psi_{ij}\rangle = \frac{1}{\sqrt{2}} (|0i\rangle + |1j\rangle), \quad (4a)$$

$$|\Phi_{ij}\rangle = \frac{1}{\sqrt{2}} (|1i\rangle + |0j\rangle), \quad (4b)$$

can be written in matrix form as

$$\hat{\rho} = \frac{1}{8} \begin{pmatrix} 1 & 1 & 0 & 0 & 0 & 0 & 0 & 0 \\ 1 & 1 & 0 & 0 & 0 & 0 & 0 & 0 \\ 0 & 0 & 1 & 1 & 0 & 0 & 0 & 0 \\ 0 & 0 & 1 & 1 & 0 & 0 & 0 & 0 \\ 0 & 0 & 0 & 0 & 1 & 1 & 0 & 0 \\ 0 & 0 & 0 & 0 & 1 & 1 & 0 & 0 \\ 0 & 0 & 0 & 0 & 0 & 0 & 1 & 1 \\ 0 & 0 & 0 & 0 & 0 & 0 & 1 & 1 \end{pmatrix}. \quad (5)$$

The QSE basis here is separable and is arranged in the order $\{|00\rangle, |11\rangle, |01\rangle, |10\rangle, |02\rangle, |13\rangle, |03\rangle, |12\rangle\}$ to highlight the block-diagonal form.

Two block structures are marked on the matrix (5). The smaller blocks (marked in red) each encompass a subspace of the Hilbert space characteristic of a single Bell-like state (4). These blocks do not fulfill our requirements, since the same environmental states can occur in different blocks, that is, $\{|0\rangle, |1\rangle\}$ in the two upper left blocks and $\{|2\rangle, |3\rangle\}$ in the lower right blocks. We will be studying density matrices where the block-diagonal form is of the type marked by the larger (blue) blocks, which encompass different subsets of the Hilbert space of the environment.

There is a fundamental difference in these two types of blocks with respect to entanglement. In the exemplary state, each smaller block encompasses a maximally entangled Bell-like state, but the mixture of two states in each larger block is separable [48], since

$$\begin{aligned} & \frac{1}{2}(|\Psi_{ij}\rangle\langle\Psi_{ij}| + |\Phi_{ij}\rangle\langle\Phi_{ij}|) \\ &= \frac{1}{2}(|+\rangle\langle+| \otimes |+\rangle\langle+| + |-\rangle\langle-| \otimes |-\rangle\langle-|), \end{aligned} \quad (6)$$

with $|\pm\rangle = 1/\sqrt{2}(|0\rangle \pm |1\rangle)$ on the QS and $|\pm\rangle = 1/\sqrt{2}(|i\rangle \pm |j\rangle)$ on the environment. Entanglement of the whole density matrix (5) depends on the interplay of the states contained in the small blocks, but it does not depend on the interplay of the states encompassed by the large blocks, since the separable form can be obtained in each of them separately.

As a central result of this paper, we will show that this result is general for the convex-roof entanglement measure defined using linear entropy of the reduced density matrix of one subsystem as the measure of pure-state entanglement and that the entanglement for any density matrix which is block diagonal in disjoint subspaces (1) is given by

$$E(\hat{\rho}) = \sum_n p_n E(\hat{\rho}_n). \quad (7)$$

Here $E(\dots)$ denotes the convex-roof entanglement measure.

III. CONVEX-ROOF ENTANGLEMENT MEASURES

We will study convex-roof entanglement measures [1,49] for bipartite mixed-state entanglement. They constitute an extension of pure-state entanglement measures to mixed states and the class of measures is defined as follows. Given a good pure-state entanglement measure such as the entropy (this can be von Neumann entropy, any of the Rényi entropies, or linear entropy) of the reduced density matrix of one of the potentially entangled subsystems, $E(|\psi\rangle)$, one can construct a mixed-state measure. This is done by first providing a decomposition of the density matrix into pure states

$$\hat{\rho} = \sum_n P_n |\psi_n\rangle\langle\psi_n|, \quad (8)$$

where P_n are probabilities and the states $|\psi_n\rangle$ do not have to be orthogonal. Note that there is an infinite number of such decompositions if the state is not pure and a full parametrization of the decompositions of a given mixed state quickly grows in complexity (and the number of free parameters) with the size

of the system [50–52]. The average of pure-state entanglement

$$\tilde{E}(\hat{\rho}) = \sum_n P_n E(|\psi_n\rangle) \quad (9)$$

is not enough to quantify entanglement of state (8), because the quantity (9) can strongly depend on the decomposition. Hence convex-roof entanglement measures are defined as the average of pure-state entanglement minimized over all possible preparations of the state (decompositions),

$$E(\hat{\rho}) = \min_{\alpha} \tilde{E}(\hat{\rho}), \quad (10)$$

where α is the set of all ensembles $\{P_n, |\psi_n\rangle\langle\psi_n|\}$ representing the state $\hat{\rho}$, as defined in Eq. (8).

IV. PROOF

We prove Eq. (7) for all density matrices of the form (1) with Eq. (2) fulfilled in three stages. We first study a QS composed of a single qubit and an environment with only two subspaces. In Sec. IV B we generalize the results to QSs of any size and in Sec. IV C we perform the simple generalization to environments with any number of subspaces.

A. Qubit and environment with two subspaces

Here we study the density matrix of a qubit (the smallest possible QS) and an environment, which has two blocks with respect to the environment. The disjoint subspaces of the environment are labeled as E_1 and E_2 and their subspaces are of dimensions N_1 and N_2 , respectively, with $N_1 + N_2 = N$, where N is the dimension of the whole environment. The density matrix can therefore be written as

$$\hat{\rho} = p_1 \hat{\rho}_1 + p_2 \hat{\rho}_2, \quad (11)$$

where p_i are probabilities with $p_1 + p_2 = 1$ and $\hat{\rho}_i$ are density matrices of nontrivial dimension $2N_i$.

We assume that the pure-state decomposition of each block that minimizes entanglement is known and we label the states by $|\phi_i^k\rangle$, where $i = 1, 2$ distinguishes between the blocks, so that

$$\hat{\rho}_i = \sum_k q_i^k |\phi_i^k\rangle\langle\phi_i^k|, \quad (12)$$

where q_i^k are probabilities, with $\sum_k q_i^k = 1$. Hence, entanglement of a given block is given by

$$E(\hat{\rho}_i) = \sum_k q_i^k E(|\phi_i^k\rangle). \quad (13)$$

We will show that there does not exist any pure-state decomposition of $\hat{\rho}$ for which entanglement is smaller than the weighed average of the entanglement present in each block, so

$$E(\hat{\rho}) = p_1 E(\hat{\rho}_1) + p_2 E(\hat{\rho}_2). \quad (14)$$

To this end we will first study entanglement of any pure state, here written as a superposition of states which belong to the distinct blocks

$$|\psi\rangle = \alpha |\psi_1\rangle + \beta |\psi_2\rangle. \quad (15)$$

These states can in turn be written as

$$|\psi_i\rangle = x_i|0\rangle \otimes |\varphi_i^0\rangle + y_i|1\rangle \otimes |\varphi_i^1\rangle. \quad (16)$$

Environmental states $|\varphi_i^0\rangle$ and $|\varphi_i^1\rangle$ do not have to be orthogonal when they belong to the same block, $\langle\varphi_i^0|\varphi_i^1\rangle \neq 0$, $i = 1, 2$, but they must be mutually orthogonal when they belong to different blocks, $\langle\varphi_a^0|\varphi_b^0\rangle = 0$, $a, b = 0, 1$.

Hence, if we rewrite the state (15) in a form which simplifies the calculation of the reduced density matrix with respect to the qubit,

$$|\psi\rangle = a|0\rangle \otimes |\psi_a\rangle + b|1\rangle \otimes |\psi_b\rangle, \quad (17)$$

the parameters are given by

$$a = \sqrt{|\alpha|^2|x_1|^2 + |\beta|^2|x_2|^2}, \quad (18a)$$

$$b = \sqrt{|\alpha|^2|y_1|^2 + |\beta|^2|y_2|^2}, \quad (18b)$$

while the normalized environmental states are

$$|\psi_a\rangle = \frac{1}{a}(\alpha x_1|\varphi_1^0\rangle + \beta x_2|\varphi_2^0\rangle), \quad (19a)$$

$$|\psi_b\rangle = \frac{1}{b}(\alpha y_1|\varphi_1^1\rangle + \beta y_2|\varphi_2^1\rangle). \quad (19b)$$

The reduced density matrix of the environment is then given by

$$\hat{\rho}_E = a^2|\psi_a\rangle\langle\psi_a| + b^2|\psi_b\rangle\langle\psi_b| \quad (20)$$

and the normalized linear entropy of the reduced density matrix, which we will use as our pure-state entanglement measure, is given by

$$E(|\psi\rangle) = 2(1 - \text{Tr}\hat{\rho}_E^2) = 4a^2b^2(1 - |\langle\psi_a|\psi_b\rangle|^2). \quad (21)$$

Since the states of the environment from different subspaces have to be orthogonal to each other, we obtain a simplified formula for the scalar product

$$|\langle\psi_a|\psi_b\rangle|^2 = \frac{1}{a^2b^2} \left| |\alpha|^2 x_1^* y_1 \langle\varphi_1^0|\varphi_1^1\rangle + |\beta|^2 x_2^* y_2 \langle\varphi_2^0|\varphi_2^1\rangle \right|^2. \quad (22)$$

We will now compare the result with the average of the (normalized) linear entropy of the block-diagonal density matrix

$$\hat{\rho}_{\text{BD}} = |\alpha|^2|\psi_1\rangle\langle\psi_1| + |\beta|^2|\psi_2\rangle\langle\psi_2|; \quad (23)$$

the matrix is a counterpart to the pure state (15), but without the interblock coherences. This is given by (the tilde signifies that this quantity is not in fact an entanglement measure, since it has not been minimized)

$$\tilde{E}(\hat{\rho}_{\text{BD}}) = |\alpha|^2 E(|\psi_1\rangle) + |\beta|^2 E(|\psi_2\rangle), \quad (24)$$

with

$$E(|\psi_i\rangle) = 4|x_i|^2|y_i|^2(1 - |\langle\varphi_i^0|\varphi_i^1\rangle|^2). \quad (25)$$

The difference between the pure-state entanglement given by Eq. (21) and the average (24) is given by

$$E(|\psi\rangle) - \tilde{E}(\hat{\rho}_{\text{BD}}) = 4|\alpha|^2|\beta|^2 \left[(|x_1|^2 - |x_2|^2)^2 + |x_1^* y_1 \langle\varphi_1^0|\varphi_1^1\rangle - x_2^* y_2 \langle\varphi_2^0|\varphi_2^1\rangle \right]^2 \geq 0. \quad (26)$$

This quantity is obviously always greater than or equal to zero, which means that the entanglement present in a superposition of states from the different blocks is always greater than the average of the entanglement contained in each block separately. Note that this result is only true because the different blocks are disjoint in terms of the states of the environment.

Given the result (26), it is now straightforward to show that entanglement present in a density matrix of the form (11) is found using Eq. (14). Let us start with an arbitrary pure-state decomposition of $\hat{\rho}$ [Eq. (8)], which we henceforth label with the index A . If we rewrite each state $|\psi_n\rangle$ as a superposition of states which belong to the distinct blocks as in Eq. (15) with coefficients α_n and β_n , we get

$$\begin{aligned} \hat{\rho} = & \sum_n P_n |\alpha_n|^2 |\psi_{1n}\rangle\langle\psi_{1n}| + \sum_n P_n |\beta_n|^2 |\psi_{2n}\rangle\langle\psi_{2n}| \\ & + \sum_n P_n \alpha_n \beta_n^* |\psi_{1n}\rangle\langle\psi_{2n}| + \sum_n P_n \alpha_n^* \beta_n |\psi_{2n}\rangle\langle\psi_{1n}|. \end{aligned} \quad (27)$$

Since the density matrix $\hat{\rho}$ is block diagonal with respect to the different subspaces, the last two terms must be equal to zero, so

$$\hat{\rho} = \hat{\rho}_B = \sum_n P_n |\alpha_n|^2 |\psi_{1n}\rangle\langle\psi_{1n}| + \sum_n P_n |\beta_n|^2 |\psi_{2n}\rangle\langle\psi_{2n}| \quad (28)$$

is a different pure-state decomposition of the same density matrix; we label this decomposition by B . The crucial difference between the two decompositions is that the latter does not contain any states which encompass both subspaces, so we can write the density matrix directly in the form given by Eq. (11) with individual decompositions,

$$\hat{\rho}_i = \frac{1}{p_i} \sum_n q_n^i |\psi_{in}\rangle\langle\psi_{in}|, \quad (29)$$

with $q_n^1 = P_n |\alpha_n|^2$, $q_n^2 = P_n |\beta_n|^2$, and $p_i = \sum_n q_n^i$. These are not necessarily the decompositions which minimize entanglement in each block separately (12).

Using the property (26), we can show that the average of the (normalized) linear entropy for decomposition A is always greater than or equal to the average for decomposition B , since

$$\begin{aligned} \tilde{E}(\hat{\rho}_A) &= \sum_n P_n E(|\psi_n\rangle) \\ &\geq \sum_n P_n |\alpha_n|^2 E(|\psi_{1n}\rangle) + \sum_n P_n |\beta_n|^2 E(|\psi_{2n}\rangle) \\ &= \tilde{E}(\hat{\rho}_B). \end{aligned} \quad (30)$$

Hence, for every pure-state decomposition of the block-diagonal density matrix $\hat{\rho}$ there exists a decomposition which does not contain superposition states between the two subspaces of the environment, for which the average of pure-state entanglement is smaller or equal. The direct consequence of this is that minimization of average entanglement over all possible pure-state decompositions will yield the average of entanglement minimized in each block separately, and mixed-state entanglement is given by Eq. (14).

B. Larger quantum system

The generalization of the result of the preceding section to a larger QS is rather straightforward. The first step is to show that pure-state entanglement is always larger than the average entanglement of the counterpart block-diagonal density matrix, meaning that the inequality

$$E(|\psi\rangle) - \tilde{E}(\hat{\rho}_{\text{BD}}) \geq 0 \quad (31)$$

still holds. Since we are still studying the situation with two subspaces, the relevant states are given by Eqs. (15) and (23), with the average linear entropy of state $\hat{\rho}_{\text{BD}}$ defined by Eq. (24). We show in the Appendix that the inequality holds.

Once this is established, we can show that for any decomposition (A) of the density matrix (8) there exists a counterdecomposition (B) which only contains states limited to either block, for which the average pure-state entanglement is smaller or equal. This is shown as in the preceding section, by writing each state in decomposition A as in Eq. (15) to obtain Eq. (27) and then by noting that the off-diagonal terms that connect the two subspaces must sum to zero, to obtain decomposition B , given by Eq. (28). As the averaged entanglement in the two decompositions can, as before, be connected using the pure-state inequality (31) yielding $\tilde{E}(\hat{\rho}_A) \geq \tilde{E}(\hat{\rho}_B)$, it follows that any convex-roof entanglement measure of a density matrix which is block diagonal in two blocks which span different environmental subspaces is given by the average entanglement contained in each block (14) regardless of QS size.

C. More subspaces

The generalization to more subspaces is even more straightforward. Obviously, since entanglement can be found by averaging the entanglement between two subspaces, if there are M block-diagonal subspaces in terms of the environment states, the entanglement of the whole density matrix can be found by averaging entanglement between one subspace and the remaining $M - 1$, while the entanglement of the $M - 1$ blocks can be found by averaging between one of them and the remaining $M - 2$, and so on. Consequently the entanglement in a matrix of M blocks can be found by averaging over the entanglement of each block and hence is given by Eq. (7).

D. Other measures of pure-state entanglement

The proof of Eq. (26) for when the QS is a qubit and the generalization of this equation for a QS of any size provided in the Appendix rely on our use of linear entropy as the base of the measure of pure-state entanglement. This is because the calculation of linear entropy does not require the knowledge of the eigenvalues of a density matrix and can thus be calculated explicitly for arbitrary matrices, even when diagonalization would require numerical evaluation.

For linear entropy, Eq. (26), regardless of QS size, is equivalent to the statement that the purity of $\hat{\rho}_E$ [Eq. (20)] and the average of in-block purities of $\hat{\rho}_{Ei} = \text{Tr}_E|\psi_i\rangle\langle\psi_i|$, $i = 1, 2$, fulfill the inequality

$$\text{Tr}\hat{\rho}_E^2 \leq |\alpha|^2\text{Tr}\hat{\rho}_{E1}^2 + |\beta|^2\text{Tr}\hat{\rho}_{E2}^2. \quad (32)$$

This means that any function which is a nonincreasing and concave function of purity will obey

$$\begin{aligned} S(\text{Tr}\hat{\rho}_E^2) &\geq S(|\alpha|^2\text{Tr}\hat{\rho}_{E1}^2 + |\beta|^2\text{Tr}\hat{\rho}_{E2}^2) \\ &\geq |\alpha|^2S(\text{Tr}\hat{\rho}_{E1}^2) + |\beta|^2S(\text{Tr}\hat{\rho}_{E2}^2). \end{aligned} \quad (33)$$

In the case of a qubit, von Neumann and the Rényi entropies are nonincreasing and concave functions of purity, so one can substitute any entanglement measure based on those entropies into Eq. (26) without any change in the inequality as long as the QS is a qubit. Hence, the whole proof holds in this case.

For larger systems the relation between purity and different entropies is more complex and it is easy to find density matrices with the same purity but different von Neumann entropies. This means that there is no direct generalization of the result obtained for linear-entropy-based pure-state entanglement measures in the situation when the QS is larger than a qubit.

V. CONSEQUENCES

In this section we discuss the consequences of the central result of this paper, namely, that the convex-roof entanglement measure based on linear entropy can be calculated using Eq. (7) for density matrices which are block diagonal in disjoint subspaces, for the theory of mixed-state entanglement. Outside the obvious simplification of calculation of the entanglement measure, since now minimization can be performed separately over parts of the QSE Hilbert space, there are two significant implications.

The first pertains to bound entanglement. Negativity [8–10], the only measure to quantify mixed-state entanglement for larger systems which can be found directly from the density matrix, is defined as the absolute sum of the negative eigenvalues of the density matrix after partial transposition with respect to one of the subsystems is performed. In other words, it is a measure based on the Peres-Horodecki criterion [53,54], which states that if the matrix after partial transposition is not a density matrix (has negative eigenvalues) then there is entanglement in the state. The drawback of the measure and the criterion is that they do not detect certain entangled states; such states are said to contain bound entanglement [11,12]. The existence of bound entanglement and its experimental demonstration have received a great deal of attention [13–17], but the exact limitations on when bound entanglement can be expected are not known, with the exception of small systems and states with additional symmetries.

For density matrices which are block diagonal with respect to disjoint subspaces of the environment, negativity can obviously be found in each block separately, since partial transposition of the density matrix with respect to the environment does not mix the blocks and both the partial transposition and the calculation of eigenstates can be done in each block separately. The following question remains: Do bound entangled states exist that transgress these blocks? Since we have shown that this property translates to a convex-roof entanglement measure, we have shown that bound entanglement will not exist between separate blocks of this type, at least not such that can be detected by a measure based on linear entropy. It can only exist within a single block, hence imposing a new

limitation on states where we can expect this type of quantum correlations.

Practically, this extends the set of states for which bound entanglement is impossible to systems of any size as long as individual disjoint blocks are not greater than 6×6 matrices. Less trivially, it also pushes the boundary for the rank of the studied bipartite state of dimension $M \times N$ required for bound entanglement [18,55], since each block can be treated separately. Hence if the dimension of the QS is M while the environment is separated into n disjoint blocks, each of dimension N_i , with $N = \sum_i N_i$, then the general criterion that guarantees only free entanglement (not bound), namely, that the rank of the density matrix has to be less than or equal to $\max(M, N)$, is supplemented by criteria for each block, which are easier to check because of the smaller size of the blocks. For bound entanglement to be impossible in a given block, its rank must be less than or equal to $\max(M, N_i)$. Note that the block criteria do not always directly imply the criterion for the full density matrix, since the dimension of a given block of the environment can be smaller than the dimension of the QS.

The second implication pertains to the existence of bipartite mixed states which are classified by convex-roof entanglement measures as containing maximum entanglement. Such states were considered unlikely by the original paper on the topic [56], but states of the required form were found in Ref. [57]. It was later shown that the periodic emergence of such states is possible in qubit-environment evolutions driven by Hamiltonians that lead to pure dephasing of the qubit [19] and are important for the emergence of objectivity [58–64]. Here we find that the emergence of such states is not limited to pure-dephasing evolutions and that they can manifest in other classes of interactions. Since there is no ambiguity between different bipartite pure-state entanglement measures in classifying states as maximally entangled, this consequence holds regardless of the measure used.

VI. RELEVANCE

The relevance of the presented proof is based on the answer to the question of whether there exist physical QSE states which have the form (1). The answer is yes and we will discuss some situations when this is the case with particular focus on thermal QSE states. In fact, the requirement for a density matrix describing a state at thermal equilibrium corresponding to temperature T , $\hat{\rho}_T = \exp(-\beta\hat{H})/Z$, with $\beta = 1/k_B T$ and Z the partition function, is that the Hamiltonian has the required form.

We will be taking into account the standard form of a Hamiltonian describing two interacting systems, so $\hat{H} = \hat{H}_{\text{QS}} + \hat{H}_E + \hat{H}_{\text{QSE}}$, where the first term describes the free Hamiltonian of the QS, the second of the environment, and the third term their interaction. We require the full Hamiltonian to be block diagonal in terms of the states of the environment. The form of the QS part is therefore arbitrary, yet the interplay of the interaction and free Hamiltonian of the environment is crucial.

There is a plethora of systems (which would here constitute the environment) for which the Hamiltonian commutes with at least one nontrivial observable \hat{A} , $[\hat{H}_E, \hat{A}] = 0$. In nontrivial

situations (when the eigenstates of the observable \hat{A} are degenerate in the full Hilbert space of \hat{H}_E or, physically speaking, the observable describes only one degree of freedom, such as spin, of a more complex system) this yields a Hamiltonian which is block diagonal in subspaces corresponding to a single eigenvalue of \hat{A} .

A good example here is the Hubbard model [65–69] as it commutes with three different operators, each reducing the dimension of the blocks. First, the Hubbard Hamiltonian commutes with the number operator, meaning that each subspace of the Hilbert space where the states describe an equal number of particles constitutes a separate block. Furthermore, the Hamiltonian commutes with the total spin \hat{S}_z component, so within each block there is a smaller block-diagonal structure, which differentiates between states with different spin symmetry. Finally, it also commutes with the parity operator, yielding even smaller nontrivial blocks. Such symmetries are common in many-body systems and are seen in, e.g., the Heisenberg, Bose-Hubbard, t - J , or Holstein models [65,70–73].

Obviously, the block-diagonal form of \hat{H}_E is not sufficient for the full Hamiltonian to demonstrate block-diagonality with respect to environmental subspaces. To this end the interaction term must possess the same symmetries as those that yield the structure of \hat{H}_E , namely, if the Hamiltonian of the environment commutes with the observable \hat{A} , then also the interaction term must commute with it, $[\hat{H}_{\text{int}}, \hat{A}] = 0$. This means that during the interaction the quantum system would be susceptible to the effect of the environment with respect to some degree of freedom while another (described by the observable \hat{A}) would not affect it.

If the Hamiltonian has the specific block-diagonal structure, not only will thermal equilibrium states retain it, but it will be kept during time evolution as long as the initial QSE state is a mixture of states contained within single blocks. The most natural situation when this is obtained is when the initial QSE state is of product form with the initial environmental state being a thermal equilibrium state of block-diagonal \hat{H}_E . There are then no limitations on the initial states of the QS.

The initial QSE state can also be used to guarantee that the block-diagonal form of the full density matrix with disjoint subspaces is kept throughout an evolution governed by a Hamiltonian where the subspaces of the blocks partially overlap. An example of such a (full) Hamiltonian is one describing a spin interacting with an environment of spins via the hyperfine interaction in the box model approximation [74–78]. Such a Hamiltonian is block diagonal in disjoint subspaces with respect to the total spin operator of the environment, but the block-diagonality which is present in subspaces governed by the projection of the total spin operator overlaps. By choosing an initial environmental state which is a mixture of states contained within these smaller subspaces, but skipping some spin quantum numbers, one could guarantee that the QSE density matrix would have the required form throughout the evolution.

VII. EXAMPLES

As an example we will study a Hamiltonian describing a qubit interacting with an environment, where the Hamiltonian

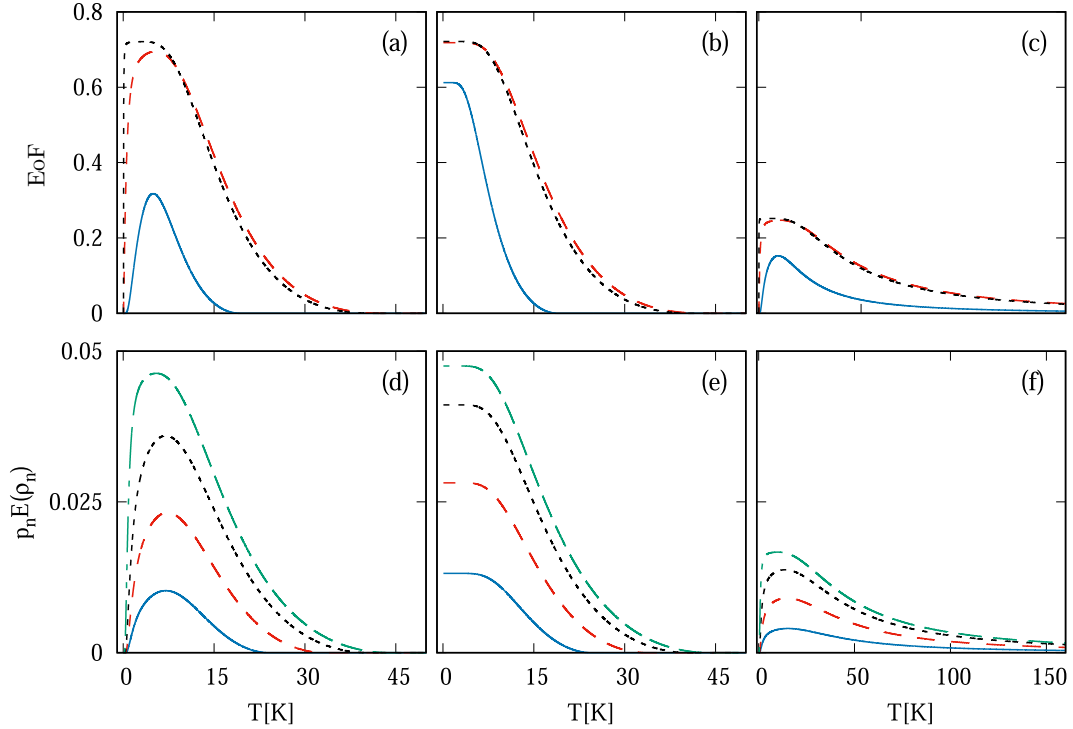


FIG. 1. Entanglement at thermal equilibrium as a function of temperature for the Hamiltonian formed from blocks given by Eq. (34). Entanglement of formation is shown for (a) finite eigenenergies E_m and nonzero magnetic field $\Omega = 1$, (b) finite eigenenergies E_m and zero magnetic field $\Omega = 0$, and (c) infinite eigenenergies $E_m = \infty$ and nonzero magnetic field $\Omega = 1$. The three curves correspond to different sizes of the environment: $K = 1$, blue solid line; $K = 10$, red dashed line; and $K = 100$, black dotted line. (d)–(f) Corresponding components of entanglement for different blocks $p_n E(\rho_n)$ for $K = 10$ with $m = -10$, blue solid line; $m = -8$, red dashed line; $m = -5$, black dotted line; and $m = 0$, green dashed line.

is block diagonal in terms of 4×4 blocks, where each block is composed of the same $|\uparrow\rangle, |\downarrow\rangle$ qubit states and of a different set of the environmental states $|m_1\rangle$ and $|m_2\rangle$. Hence each block is given in the QSE basis $\{|\uparrow m_1\rangle, |\uparrow m_2\rangle, |\downarrow m_1\rangle, |\downarrow m_2\rangle\}$ and the different blocks are distinguished by quantum number m . We limit the size of the blocks so that we can use the Wootters formula for two qubits to quantify the entanglement of formation [29] in each block while studying the different possible thermal behaviors of the entanglement of the whole state. Since the QS is a qubit, we can use entanglement of formation even though it is based of von Neumann entropy, as shown in Sec. IV D.

We study a Hamiltonian that is composed of blocks given by

$$\hat{H}^m = \begin{pmatrix} E_{m1} & 0 & 0 & M_m \\ 0 & E_m & 0 & 0 \\ 0 & 0 & E_m & 0 \\ M_m^* & 0 & 0 & E_{m2} \end{pmatrix}, \quad (34)$$

so the full Hamiltonian is $\hat{H} = \sum_m \hat{H}^m$. The blocks are intentionally chosen in such a way that they have two entangled eigenstates and two separable ones. The Hamiltonian parameters are

$$E_{m1} = \alpha \left(m + \frac{\Omega}{2} \right), \quad (35a)$$

$$E_{m2} = -\alpha \left(m + 1 + \frac{\Omega}{2} \right), \quad (35b)$$

$$M_m = \alpha \sqrt{K(K+1) - m(m+1)}, \quad (35c)$$

mimicking spin systems, with $m = 0, \pm 1, \pm 2, \dots, \pm K$, where $K = \max(m)$ is an integer. The parameter $\alpha = 1/\sqrt{K}$ eV is responsible for the strength of the QSE interaction. The scaling with \sqrt{K} is responsible for the interaction with the whole environment being equivalent regardless of K for large values of K , which is in accordance with the scaling prevalent for quantum-dot spin qubits [76,78]. The parameter Ω plays the role of the magnetic field. The E_m denote the energies of the separable eigenstates.

In Figs. 1(a)–1(c) we plot the EoF between the qubit and the environment at thermal equilibrium as a function of temperature for the Hamiltonian. The figures correspond to three sets of Hamiltonian parameters which lead to qualitatively different behavior of entanglement. Figures 1(a) and 1(b) have separable eigenenergy specified as $E_m = \frac{1}{2}(E_{m1} + E_{m2})$, meaning that within a single block the entangled eigenstates constitute the ground state and the state with the highest energy. For Fig. 1(a) the magnetic-field parameter $\Omega = 1$ is nonzero, lifting the degeneracy between the blocks, while for Fig. 1(b) $\Omega = 0$, which leads to degenerate eigenstates (all four eigenstates within a given block have no m dependence). In Fig. 1(c) we have $\Omega = 1$ as in Fig. 1(a), but the separable eigenstates are much higher in energy, $E_m = \infty$, which means

that the Hamiltonian effectively has two-dimensional blocks. The three curves on each plot correspond to $K = 1$ with 3 blocks (blue solid line), $K = 10$ with 21 blocks (red dashed line), and $K = 100$ with 201 blocks (black dotted line).

Figure 1(a) shows a fast growth of entanglement followed by slower decay which is cut short by sudden death [79–82] and beyond a certain temperature there is no entanglement. The rate of the growth strongly depends on the number of blocks, so the difference between the $K = 10$ and $K = 100$ curves is obvious only on the low-temperature side. There is no entanglement at zero temperature; this is easy to understand since the ground state of the whole Hamiltonian is the lowest-energy state of the $m = K$ block, which is separable, since $M_K = 0$. Figure 1(d) contains the temperature dependence of a choice of components which correspond to different blocks in the whole EoF curve for $K = 10$ [the probability of a given block times the EoF within the block as in Eq. (7)]. It is interesting to note that sudden death occurs at different temperatures for different components, which should yield points in the corresponding full entanglement curve which are not smooth. These points are not visible because the sudden death resulting from the rising mixedness of the Gibbs state with temperature occurs much more gently (although undeniably it is present) than seen typically in evolution [81,83–86].

Figures 1(b) and 1(e) correspond to a situation where there is a degenerate ground state showing entanglement of the full state and its components, respectively. The lowest-energy state of each block is also the ground state of the Hamiltonian; since these states are entangled (with the exception of the $m = K$ state), the zero-temperature state is a mixture of entangled states from different blocks and is itself entangled. With rising temperature we only observe a decay of entanglement corresponding to the state of an individual block becoming mixed. The decay is again not exponential due to sudden death which occurs at some finite temperature.

Note that the striking qualitative difference between the temperature dependences of entanglement in Figs. 1(a) and 1(b) is not a result of different entanglement behavior within the blocks. In fact, the blocks in both cases behave qualitatively the same, but the probabilities with which the entanglement of a given block contributes to overall entanglement are very different in the two cases. The results of Fig. 1(a) show a tradeoff between the rising probability of a given block to occur within the Gibbs state versus entanglement becoming smaller when the state becomes more mixed, while in the results of Fig. 1(b) the diminishing of entanglement closely follows the decay of entanglement within the blocks.

This changes in Figs. 1(c) and 1(f), where the blocks of the Hamiltonian are effectively two dimensional, which leads to sudden-death-type behavior being impossible due to the geometry of separable states [83,87,88]. The situation is equivalent to that of Fig. 1(a) with the exception that only two eigenstates within each block, the entangled ones, are parts of the Gibbs state. This leads to no sudden death in the components and therefore no sudden death in the entanglement of the full state, so actual separability is reached only at infinite temperature. There is also an obvious effect visible in the maximum entanglement which can be present at thermal

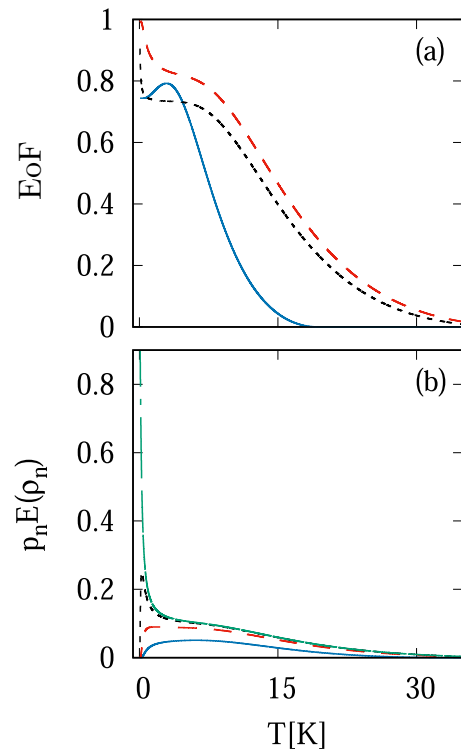


FIG. 2. Entanglement of formation as a function of temperature T for finite eigenenergies E_m and nonzero magnetic field $\Omega = 1$, considering only nonpositive values of m . The parameters for (a) and (b) are the same as in Figs. 1(a)–1(c) and 1(d)–1(f), respectively.

equilibrium, which is much smaller. This is because mixing of two orthogonal entangled states which are confined to the same two-dimensional subspace is much more detrimental to entanglement than the admixture of separable states. Hence here, although the probabilities with which the blocks are mixed behave very similarly to that in Fig. 1(a), it is the different temperature dependence in individual blocks that leads to qualitatively different results.

In Fig. 2 we show the same situation as in Fig. 1(a), but where only blocks with nonpositive values of m have been taken into account. This eliminates the block with $m = K$, which has only separable eigenstates and also contains the ground state of the whole Hamiltonian. Now the ground state is also entangled, which leads to a more complicated tradeoff situation between the components shown in Fig. 2(b) starting with an entangled Gibbs state at zero temperature. The corresponding component of entanglement decays very rapidly with temperature, while all other components start to grow, which leads to a plateau at small temperatures for larger K and an initial growth of entanglement for $K = 1$.

We have shown that the temperature dependence of entanglement can be very diverse even in the case of the simple Hamiltonian which has been studied. This fact is obvious in terms of possible behavior within a given block of the density matrix, but our study shows that the interplay of probabilities pertaining to each block can be just as important. By changing the way that temperature mixes the different blocks in the Gibbs state, we have obtained three qualitatively different scenarios, varying not only in zero-temperature entanglement,

but also in monotonicity for different temperature regimes. It is important to note that the curves were obtained by qualitatively the same Hamiltonian, and a larger change was necessary only to modify the behavior of entanglement within a single block.

VIII. CONCLUSION

We have supplied a proof that the convex-roof entanglement measure based on linear entropy is the average over entanglement within a given block of a density matrix which is block diagonal in such a way that individual blocks are contained within different subspaces of one of two potentially entangled subsystems (say, the environment). Although this may seem to be an overly specific regime of application, there are many Hamiltonians which possess this quality. For such Hamiltonians, any thermal-equilibrium state will inherit the same quality and the simplification of resulting calculation of entanglement can be immense. If an initial bipartite state is also block diagonal in such a way, then the evolution driven by the Hamiltonian will yield a state which retains the necessary form at any given time.

We have used the method to find the temperature dependence of entanglement in a Gibbs state of a large system, the Hamiltonian of which is composed of a multitude of small blocks. This allowed us to show four very different behaviors of entanglement which can occur in different parameter ranges. These behaviors can depend on how entanglement reacts to the temperature change within each block and on the way that different blocks are mixed. We have shown that the interplay of probabilities can yield striking differences in the trends of entanglement, both in terms of entanglement at zero temperature and whether it is ascending or descending in a given temperature range. Temperature-driven sudden-death-type behavior is the singular property which requires sudden-death behavior to occur within each block separately.

On the more quantum-theoretical side, our proof allows us to infer that bound entanglement cannot traverse multiple blocks; it is possible only within a single block. This has consequences for the calculation of measures such as negativity, which cannot detect bound entanglement, making them more reliable.

ACKNOWLEDGMENT

This work was supported by Project No. 20-16577S of the Czech Science Foundation.

APPENDIX: QUDIT AND ENVIRONMENT WITH TWO SUBSPACES

Here we will show that entanglement of any pure state that contains coherences between subspaces of the environment

[Eq. (15)] is greater than or equal to the average entanglement in its block-diagonal counterpart [Eq. (23)] regardless of the size of the QS. Since we are now dealing with a qudit, a system of dimension K , the states (16) have to be replaced by

$$|\psi_i\rangle = \sum_s x_i^s |s\rangle \otimes |\varphi_i^s\rangle, \quad (\text{A1})$$

where the summation over s spans the qudit Hilbert space and the states $|s\rangle$ are a set of basis states on the QS; $i = 1, 2$ still differentiates between the subspaces of the environment. This yields the qudit version of Eq. (17),

$$|\psi\rangle = \sum_s a_s |s\rangle \otimes |\psi_s\rangle, \quad (\text{A2})$$

with

$$a_s = \sqrt{|\alpha|^2 |x_1^s|^2 + |\beta|^2 |x_2^s|^2} \quad (\text{A3})$$

and

$$|\psi_s\rangle = \frac{1}{a_s} (\alpha x_1^s |\varphi_1^s\rangle + \beta x_2^s |\varphi_2^s\rangle). \quad (\text{A4})$$

The reduced density matrix of the environment is given by

$$\hat{\rho}_E = \sum_s a_s^2 |\psi_s\rangle \langle \psi_s| \quad (\text{A5})$$

and the normalized linear entropy of the reduced density matrix is

$$E(|\psi\rangle) = 4 \sum_{s \neq s'} a_s^2 a_{s'}^2 (1 - |\langle \psi_s | \psi_{s'} \rangle|^2). \quad (\text{A6})$$

Since the states of the environment from different subspaces have to be orthogonal to each other, the simplified formula for the scalar product is still valid and we have

$$|\langle \psi_s | \psi_{s'} \rangle|^2 = \frac{1}{a_s^2 a_{s'}^2} \left| |\alpha|^2 x_1^{s*} x_1^{s'} \langle \varphi_1^s | \varphi_1^{s'} \rangle + |\beta|^2 x_2^{s*} x_2^{s'} \langle \varphi_2^s | \varphi_2^{s'} \rangle \right|^2. \quad (\text{A7})$$

The average of the linear entropy of the block-diagonal density matrix (23) is still given by Eq. (24), but with

$$E(|\psi_i\rangle) = 4 \sum_{s \neq s'} |x_i^s|^2 |x_i^{s'}|^2 (1 - |\langle \varphi_i^s | \varphi_i^{s'} \rangle|^2). \quad (\text{A8})$$

Since the formulas in both cases only differ by an identical sum over different qudit basis states, it follows that the formula (14) holds for a QS of any size.

- [1] M. B. Plenio and S. Virmani, An introduction to entanglement measures, *Quantum Inf. Comput.* **7**, 1 (2007).
 [2] C. H. Bennett, D. P. DiVincenzo, J. A. Smolin, and W. K. Wootters, Mixed-state entanglement and quantum error correction, *Phys. Rev. A* **54**, 3824 (1996).

- [3] V. Vedral, M. B. Plenio, M. A. Rippin, and P. L. Knight, Quantifying Entanglement, *Phys. Rev. Lett.* **78**, 2275 (1997).
 [4] E. M. Rains, Rigorous treatment of distillable entanglement, *Phys. Rev. A* **60**, 173 (1999).

- [5] J. Eisert, T. Felbinger, P. Papadopoulos, M. B. Plenio, and M. Wilkens, Classical Information and Distillable Entanglement, *Phys. Rev. Lett.* **84**, 1611 (2000).
- [6] P. M. Hayden, M. Horodecki, and B. M. Terhal, The asymptotic entanglement cost of preparing a quantum state, *J. Phys. A: Math. Gen.* **34**, 6891 (2001).
- [7] C. H. Bennett, G. Brassard, S. Popescu, B. Schumacher, J. A. Smolin, and W. K. Wootters, Purification of Noisy Entanglement and Faithful Teleportation via Noisy Channels, *Phys. Rev. Lett.* **76**, 722 (1996).
- [8] G. Vidal and R. F. Werner, Computable measure of entanglement, *Phys. Rev. A* **65**, 032314 (2002).
- [9] J. Lee, M. Kim, Y. Park, and S. Lee, Partial teleportation of entanglement in a noisy environment, *J. Mod. Opt.* **47**, 2151 (2000).
- [10] M. B. Plenio, Logarithmic Negativity: A Full Entanglement Monotone That is not Convex, *Phys. Rev. Lett.* **95**, 090503 (2005).
- [11] P. Horodecki, Separability criterion and inseparable mixed states with positive partial transposition, *Phys. Lett. A* **232**, 333 (1997).
- [12] M. Horodecki, P. Horodecki, and R. Horodecki, Mixed-State Entanglement and Distillation: Is there a “Bound” Entanglement in Nature? *Phys. Rev. Lett.* **80**, 5239 (1998).
- [13] J. A. Smolin, Four-party unlockable bound entangled state, *Phys. Rev. A* **63**, 032306 (2001).
- [14] J. DiGuglielmo, A. Sambrowski, B. Hage, C. Pineda, J. Eisert, and R. Schnabel, Experimental Unconditional Preparation and Detection of a Continuous Bound Entangled State of Light, *Phys. Rev. Lett.* **107**, 240503 (2011).
- [15] B. C. Hiesmayr and W. Löffler, Complementarity reveals bound entanglement of two twisted photons, *New J. Phys.* **15**, 083036 (2013).
- [16] G. Sentís, J. N. Greiner, J. Shang, J. Siewert, and M. Kleinmann, Bound entangled states fit for robust experimental verification, *Quantum* **2**, 113 (2018).
- [17] A. Gabdulin and A. Mandilara, Investigating bound entangled two-qutrit states via the best separable approximation, *Phys. Rev. A* **100**, 062322 (2019).
- [18] P. Horodecki, M. Lewenstein, G. Vidal, and I. Cirac, Operational criterion and constructive checks for the separability of low-rank density matrices, *Phys. Rev. A* **62**, 032310 (2000).
- [19] K. Roszak, Measure of qubit-environment entanglement for pure dephasing evolutions, *Phys. Rev. Res.* **2**, 043062 (2020).
- [20] X. Wang and M. M. Wilde, Cost of Quantum Entanglement Simplified, *Phys. Rev. Lett.* **125**, 040502 (2020).
- [21] B. Bergh and M. Gärtner, Experimentally Accessible Bounds on Distillable Entanglement from Entropic Uncertainty Relations, *Phys. Rev. Lett.* **126**, 190503 (2021).
- [22] K. Roszak and L. Cywiński, Characterization and measurement of qubit-environment-entanglement generation during pure dephasing, *Phys. Rev. A* **92**, 032310 (2015).
- [23] K. Roszak and L. Cywiński, Equivalence of qubit-environment entanglement and discord generation via pure dephasing interactions and the resulting consequences, *Phys. Rev. A* **97**, 012306 (2018).
- [24] K. Roszak, Criteria for system-environment entanglement generation for systems of any size in pure-dephasing evolutions, *Phys. Rev. A* **98**, 052344 (2018).
- [25] K. Roszak, D. Kwiatkowski, and L. Cywiński, How to detect qubit-environment entanglement generated during qubit dephasing, *Phys. Rev. A* **100**, 022318 (2019).
- [26] M. Strzałka, D. Kwiatkowski, L. Cywiński, and K. Roszak, Qubit-environment negativity versus fidelity of conditional environmental states for a nitrogen-vacancy-center spin qubit interacting with a nuclear environment, *Phys. Rev. A* **102**, 042602 (2020).
- [27] M. Strzałka and K. Roszak, Detection of entanglement during pure dephasing evolutions for systems and environments of any size, *Phys. Rev. A* **104**, 042411 (2021).
- [28] X. Zhan, D. Qu, K. Wang, L. Xiao, and P. Xue, Experimental detection of qubit-environment entanglement without accessing the environment, *Phys. Rev. A* **104**, L020201 (2021).
- [29] W. K. Wootters, Entanglement of Formation of an Arbitrary State of Two Qubits, *Phys. Rev. Lett.* **80**, 2245 (1998).
- [30] K. Audenaert, F. Verstraete, and B. De Moor, Variational characterizations of separability and entanglement of formation, *Phys. Rev. A* **64**, 052304 (2001).
- [31] G. Tóth, T. Moroder, and O. Gühne, Evaluating Convex Roof Entanglement Measures, *Phys. Rev. Lett.* **114**, 160501 (2015).
- [32] C. Zhang, S. Yu, Q. Chen, H. Yuan, and C. H. Oh, Evaluation of entanglement measures by a single observable, *Phys. Rev. A* **94**, 042325 (2016).
- [33] T. M. Carrijo, W. B. Cardoso, and A. T. Avelar, Linear semi-infinite programming approach for entanglement quantification, *Phys. Rev. A* **104**, 022413 (2021).
- [34] B. M. Terhal and K. G. H. Vollbrecht, Entanglement of Formation for Isotropic States, *Phys. Rev. Lett.* **85**, 2625 (2000).
- [35] G. Giedke, M. M. Wolf, O. Krüger, R. F. Werner, and J. I. Cirac, Entanglement of Formation for Symmetric Gaussian States, *Phys. Rev. Lett.* **91**, 107901 (2003).
- [36] S. Ryu, S.-S. B. Lee, and H.-S. Sim, Minimax optimization of entanglement witness operator for the quantification of three-qubit mixed-state entanglement, *Phys. Rev. A* **86**, 042324 (2012).
- [37] B. Regula and G. Adesso, Entanglement Quantification Made Easy: Polynomial Measures Invariant under Convex Decomposition, *Phys. Rev. Lett.* **116**, 070504 (2016).
- [38] B. Röthlisberger, J. Lehmann, and D. Loss, Numerical evaluation of convex-roof entanglement measures with applications to spin rings, *Phys. Rev. A* **80**, 042301 (2009).
- [39] S. Ryu, W. Cai, and A. Caro, Quantum entanglement of formation between qudits, *Phys. Rev. A* **77**, 052312 (2008).
- [40] S. Allende, D. Altbir, and J. C. Retamal, Simulated annealing and entanglement of formation for $(n \otimes m)$ -dimensional mixed states, *Phys. Rev. A* **92**, 022348 (2015).
- [41] K. Życzkowski, Volume of the set of separable states. II, *Phys. Rev. A* **60**, 3496 (1999).
- [42] V. M. Akulin, G. A. Kabatiansky, and A. Mandilara, Essentially entangled component of multipartite mixed quantum states, its properties, and an efficient algorithm for its extraction, *Phys. Rev. A* **92**, 042322 (2015).
- [43] D. Markham, J. Anders, V. Vedral, M. Muraio, and A. Miyake, Survival of entanglement in thermal states, *Europhys. Lett.* **81**, 40006 (2008).

- [44] Y. Li, D. E. Browne, L. C. Kwek, R. Raussendorf, and T.-C. Wei, Thermal States as Universal Resources for Quantum Computation with Always-On Interactions, *Phys. Rev. Lett.* **107**, 060501 (2011).
- [45] C. Weedbrook, S. Pirandola, and T. C. Ralph, Continuous-variable quantum key distribution using thermal states, *Phys. Rev. A* **86**, 022318 (2012).
- [46] J. Wu and T. H. Hsieh, Variational Thermal Quantum Simulation via Thermofield Double States, *Phys. Rev. Lett.* **123**, 220502 (2019).
- [47] M. Motta, C. Sun, A. T. Tan, M. J. O'Rourke, E. Ye, A. J. Minnich, F. G. Brandão, and G. K.-L. Chan, Determining eigenstates and thermal states on a quantum computer using quantum imaginary time evolution, *Nat. Phys.* **16**, 205 (2020).
- [48] W.-C. Su, K.-P. Chen, M.-C. Tsai, and Z.-Y. Su, A decomposition method for the bipartite separability of Bell diagonal states, *Int. J. Nucl. Quantum Eng.* **5**, 624 (2011).
- [49] G. Vidal, Entanglement monotones, *J. Mod. Opt.* **47**, 355 (2000).
- [50] M. A. Nielsen and I. L. Chuang, *Quantum Computation and Quantum Information* (Cambridge University Press, Cambridge, 2000).
- [51] L. Gurvits, *Proceedings of the Thirty-Fifth Annual ACM Symposium on Theory of Computing, San Diego, 2003* (Association for Computing Machinery, New York, 2003), pp. 10–19.
- [52] L. Gurvits, Classical complexity and quantum entanglement, *J. Comput. Syst. Sci.* **69**, 448 (2004), special issue on STOC 2003, edited by S. Khanna and A. Srinivasan.
- [53] A. Peres, Separability Criterion for Density Matrices, *Phys. Rev. Lett.* **77**, 1413 (1996).
- [54] M. Horodecki, P. Horodecki, and R. Horodecki, Separability of mixed states: Necessary and sufficient conditions, *Phys. Lett. A* **223**, 1 (1996).
- [55] B. Kraus, J. I. Cirac, S. Karnas, and M. Lewenstein, Separability in $2 \times N$ composite quantum systems, *Phys. Rev. A* **61**, 062302 (2000).
- [56] D. Cavalcanti, F. G. S. L. Brandão, and M. O. Terra Cunha, Are all maximally entangled states pure? *Phys. Rev. A* **72**, 040303(R) (2005).
- [57] Z.-G. Li, M.-J. Zhao, S.-M. Fei, H. Fan, and W. M. Liu, Mixed maximally entangled states, *Quantum Inf. Comput.* **12**, 63 (2012).
- [58] H. Ollivier, D. Poulin, and W. H. Zurek, Objective Properties from Subjective Quantum States: Environment as a Witness, *Phys. Rev. Lett.* **93**, 220401 (2004).
- [59] H. Ollivier, D. Poulin, and W. H. Zurek, Environment as a witness: Selective proliferation of information and emergence of objectivity in a quantum universe, *Phys. Rev. A* **72**, 042113 (2005).
- [60] W. H. Zurek, Quantum Darwinism, *Nat. Phys.* **5**, 181 (2009).
- [61] J. K. Korbicz, P. Horodecki, and R. Horodecki, Objectivity in a Noisy Photonic Environment through Quantum State Information Broadcasting, *Phys. Rev. Lett.* **112**, 120402 (2014).
- [62] R. Horodecki, J. K. Korbicz, and P. Horodecki, Quantum origins of objectivity, *Phys. Rev. A* **91**, 032122 (2015).
- [63] K. Roszak and J. K. Korbicz, Entanglement and objectivity in pure dephasing models, *Phys. Rev. A* **100**, 062127 (2019).
- [64] D. Kwiatkowski, Ł. Cywiński, and J. K. Korbicz, Appearance of objectivity for NV centers interacting with dynamically polarized nuclear environment, *New J. Phys.* **23**, 043036 (2021).
- [65] T. Giamarchi and O. U. Press, *Quantum Physics in One Dimension* (Clarendon, Oxford, 2004).
- [66] J. Hubbard and B. H. Flowers, Electron correlations in narrow energy bands, *Proc. R. Soc. London Ser. A* **276**, 238 (1963).
- [67] M. Rasetti, *The Hubbard Model* (World Scientific, Singapore, 1991).
- [68] S. A. Jafari, Introduction to Hubbard model and exact diagonalization, *Iran. J. Phys. Res.* **8**, 113 (2008).
- [69] *The Hubbard Model: Its Physics and Mathematical Physics*, edited by D. Baeriswyl, D. K. Campbell, J. M. P. Carmelo, F. Guinea, and E. Louis, NATO Advanced Studies Institute, Series B: Physics (Springer, New York, 2013), Vol. 343.
- [70] G. D. Mahan, *Many-Particle Physics* (Kluwer, New York, 2000).
- [71] H. A. Gersch and G. C. Knollman, Quantum cell model for bosons, *Phys. Rev.* **129**, 959 (1963).
- [72] E. Dagotto and A. Moreo, Exact diagonalization study of the frustrated Heisenberg model: A new disordered phase, *Phys. Rev. B* **39**, 4744 (1989).
- [73] T. Sowiński, Exact diagonalization of the one-dimensional Bose-Hubbard model with local three-body interactions, *Phys. Rev. A* **85**, 065601 (2012).
- [74] I. A. Merkulov, A. L. Efros, and M. Rosen, Electron spin relaxation by nuclei in semiconductor quantum dots, *Phys. Rev. B* **65**, 205309 (2002).
- [75] A. Melikidze, V. V. Dobrovitski, H. A. De Raedt, M. I. Katsnelson, and B. N. Harmon, Parity effects in spin decoherence, *Phys. Rev. B* **70**, 014435 (2004).
- [76] E. Barnes, L. Cywiński, and S. Das Sarma, Master equation approach to the central spin decoherence problem: Uniform coupling model and role of projection operators, *Phys. Rev. B* **84**, 155315 (2011).
- [77] A. V. Shumilin and D. S. Smirnov, Nuclear Spin Dynamics, Noise, Squeezing, and Entanglement in Box Model, *Phys. Rev. Lett.* **126**, 216804 (2021).
- [78] P. Mazurek, K. Roszak, R. W. Chhajlany, and P. Horodecki, Sensitivity of entanglement decay of quantum-dot spin qubits to the external magnetic field, *Phys. Rev. A* **89**, 062318 (2014).
- [79] A. K. Rajagopal and R. W. Rendell, Decoherence, correlation, and entanglement in a pair of coupled quantum dissipative oscillators, *Phys. Rev. A* **63**, 022116 (2001).
- [80] K. Życzkowski, P. Horodecki, M. Horodecki, and R. Horodecki, Dynamics of quantum entanglement, *Phys. Rev. A* **65**, 012101 (2001).
- [81] T. Yu and J. H. Eberly, Finite-Time Disentanglement Via Spontaneous Emission, *Phys. Rev. Lett.* **93**, 140404 (2004).
- [82] T. Yu and J. Eberly, Sudden death of entanglement, *Science* **323**, 598 (2009).
- [83] K. Roszak and P. Machnikowski, Complete disentanglement by partial pure dephasing, *Phys. Rev. A* **73**, 022313 (2006).
- [84] M. I. Shaukat, E. V. Castro, and H. Terças, Entanglement sudden death and revival in quantum dark-soliton qubits, *Phys. Rev. A* **98**, 022319 (2018).
- [85] F. Wang, P.-Y. Hou, Y.-Y. Huang, W.-G. Zhang, X.-L. Ouyang, X. Wang, X.-Z. Huang, H.-L. Zhang, L. He, X.-Y. Chang, and

- L.-M. Duan, Observation of entanglement sudden death and rebirth by controlling a solid-state spin bath, *Phys. Rev. B* **98**, 064306 (2018).
- [86] S. Chakraborty and A. K. Sarma, Delayed sudden death of entanglement at exceptional points, *Phys. Rev. A* **100**, 063846 (2019).
- [87] K. Życzkowski, P. Horodecki, A. Sanpera, and M. Lewenstein, Volume of the set of separable states, *Phys. Rev. A* **58**, 883 (1998).
- [88] I. Bengtsson and K. Życzkowski, *Geometry of Quantum States: An Introduction to Quantum Entanglement* (Cambridge University Press, Cambridge, 2006).